Journal of the Korean Nuclear Society
Volume 25, Number 2, June 1993

The Effect of Tributary Pipe Breaks on the Core Support Barrel Shell Responses

Myung Jo Jhung
Korea Atomic Energy Research Institute

Won Gul Hwang
Chonnam National University

(Received September 26, 1992)

분기관파단이 노심지지배럴의 쉘응답에 미치는 영향

정명조
한국원자력연구소

황원걸
전남대학교

(1992. 9. 26 접수)

Abstract

Work on fracture mechanics has provided a technical basis for elimination of main coolant loop double ended guillotine breaks from the structural design basis of reactor coolant system. Without main coolant loop pipe breaks, the tributary pipe breaks must be considered as design bases until further fracture mechanics work could eliminate some of these breaks from design consideration. This paper determines the core support barrel shell responses for the 3 inch pressurizer spray line nozzle break which is expected to be the only inlet break remaining in the primary side after leak-before-break evaluation is extended to smaller size pipes in the near future. The responses are compared with those due to 14 inch safety injection nozzle break and main coolant loop pipe break. The results show that, when the leak-before-break concept is applied to the primary side piping systems with a diameter of 10 inches or over, the core support barrel shell responses due to pipe breaks in the primary side are negligible for the faulted condition design.

요 약

본 논문은 원자력발전소의 배관설계에 파단전 누설(leak-before-break : LBB) 개념이 적용됨에 따라 새롭게 해석대상이 된 분기관파단에 의한 노심지지배럴의 쉘응답을 계산한 것이다. 앞으로 직경 10인치 이상의 고에너지 배관에 대해 LBB 개념이 적용될 것으로 예상되는 바, 이 경우 LBB

적용대상에서 제외되는 유일한 1차측 배관인 3인치 가압기 분무관의 파단을 가정하였고 이때 노심지지배럴에 가해지는 쉘응답을 구하였다. 이들 응답을 직경 10인치 이상인 배관파단시의 응답과 비교한 결과 앞으로 직경 10인치 이상의 배관에 대해 LBB개념이 적용될 경우 배관파단에 대한 노심지지배럴의 쉘응답은 무시할 수 있음을 보였다.

1. Introduction

The core support barrel(CSB), the major structural member of the reactor internals, is a right circular cylinder including a heavy external ring flange at the top end and an internal ring flange at the lower end(Fig.1). It is supported from a ledge on the reactor vessel and, in turn, supports the lower support structure upon which the fuel assemblies rest. Since the weight of the CSB is supported at its upper end, it is possible that coolant flow could induce vibrations in the structure. Therefore, amplitude limiting devices, or snubbers, are installed on the outside of the CSB near the bottom end. It is classified as a core support structure by ASME Code Class and so should be designed to meet the Level D service limits defined in ASME Code Section III(Ref.1). The pipe break load is one of the service loadings making up Level D conditions.

During an inlet pipe break, a series of pressure waves propagate throughout the reactor. Among other effects, these pressure waves produce a loading on CSB, the result of which is a major internal pressure pulse. The CSB consisting of upper flange, barrel cylinder and lower flange is treated as axisymmetric thin shells whose total response is the combination of responses due to beam and shell harmonics. Generally the responses of beam harmonics come from the analysis of coupled internals and core where CSB is treated as beam. The responses of shell harmonics are determined separately using the thin shell elements. The beam stress and shell stress are combined to yield the total CSB stresses due to pipe break and these values are compared with the code allowables.

This paper determines the CSB shell responses such as maximum stresses and stress intensities in the barrel for the 3 inch pressurizer spray line nozzle break. Also, the responses for the 3 inch break are compared with those of main coolant loop pipe break (350 in^2 inlet pipe break at full

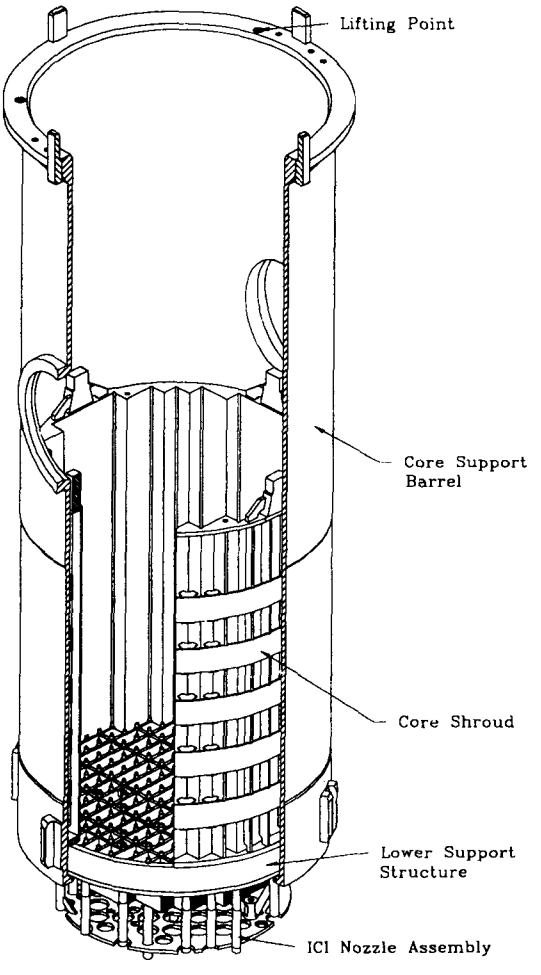

Fig. 1. Core Support Barrel Assembly

power operating condition) and 14 inch safety injection nozzle break which are not considered as design basis any more.

2. Tributary Pipe Breaks

In the recent design of nuclear power plants, main coolant loop double ended guillotine breaks are eliminated from the design basis because of leak-before-break concept. Instead branch line pipe breaks are considered as one of the Level D service loadings. Of the pipe breaks postulated, leak-before-break evaluation is being performed for piping systems with a diameter of 10 inches or over and it is anticipated that pipe breaks with a diameter of 10 inches or over not be considered as design basis any more. In this case, only the 3 inch pressurizer spray line nozzle break remains in the design basis in the primary side. Therefore this break is considered as design basis though all other high energy piping systems with a diamerter of 10 inches or over are eliminated from design basis pipe break. The responses for 14 inch safety injection nozzle break are obtained in this paper for the comparison purpose only.

3. Response Analysis

3.1. Model

The CSB may be idealized as an assembly of discrete structural elements. The axisymmetric nature of the CSB and the finite element requirement suggest that conical shell segments joined at their nodal point circles be used. The determination of the axial length of the segments is bounded on the lower limit by the nodal capacity of the finite element and on the upper limit by the shell decay length. The shell decay length is from Ref.2

$$L_c = \pi\left[\frac{3(1-v^2)}{a^2 \times h^2}\right]^{-\frac{1}{4}}$$

where a=mean shell radius(inch),
h=mean shell thickness(inch),
v=Poisson's ratio.

For the CSB considered in this paper a=70.5 inch, h=3.0 inch and v=0.3

$$L_c = \pi\left[\frac{3(1-0.3^2)}{70.5^2 \times 3.0^2}\right]^{-\frac{1}{4}} = 35.5 \text{ inch}$$

Using these considerations, the model is developed and it has 112 nodes and 111 shell segments(Fig.2) where the shorter segments are used at the flanges and at the step changes in the thickness of the barrel.

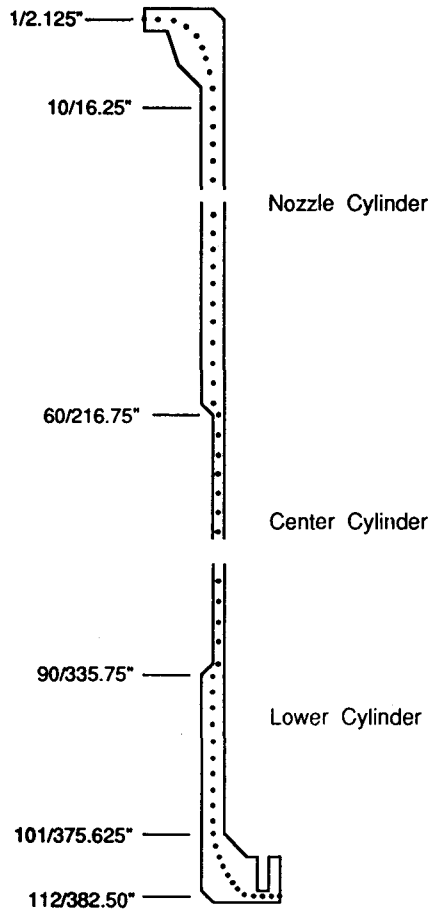

Fig. 2. CSB Finite Element Model (Node Number/Elevation)

The weight of the major internals components in the CSB lower flange region is considered. The weight is actually an axial force applied to the lower flange and is considered as a mass which modifies the structural mass of the several elements of lower flange. The major internals components supported by the CSB lower flange are the fuel assemblies, core support plate, lower support structure and core shroud. The additional mass of these components is combined with the structural mass of the flange elements 107 through 111 (Fig.2). The center of gravity for this mass is well above the lower flange and the effective additional weight acting on the flange is conservatively taken as one-half of this weight. But it is noted that this additional mass will have little effect on the CSB dynamic response because of lower flange constraints.

The boundary conditions imposed on the finite element model attempt to simulate the restraints on the CSB in its actual physical environment. At the upper flange, the restraining factors, such as reactor vessel head, hold down ring preload and upper guide structure upper flange, preclude the possibility of motion in the axial, radial and tangential directions. But there is no restriction on the relative rotation in the vertical plane between the upper guide structure and CSB upper flanges. To simulate this condition, one node of upper flange is fixed axially, radially and tangentially, but permitted to rotate. The snubbers restrain several nodes from displacing in the tangential direction. Therefore, nodes within snubber elevation are fixed tangentially. The lower flange is fixed radially and tangentially. The boundary conditions at the lower flange are fulfilled by restraining one node of lower flange radially and tangentially.

3.2. Equations of Motion

If a viscous damping is assumed, the force equilibrium equations may be expressed as

$$[M]\{\ddot{X}\} + [C]\{\dot{X}\} + [K]\{X\} = \{P(t)\} \quad (1)$$

where $[M]$: mass matrix
$[C]$: damping matrix
$[K]$: stiffness matrix
$\{\ddot{X}\}$: acceleration vector
$\{\dot{X}\}$: velocity vector
$\{X\}$: displacement vector
$\{P(t)\}$: load vector.

The equation of motion may be solved numerically by step-by-step integration procedure (Ref.3). The only practical way of solving the set of second order ordinary differential equations with arbitrary forcing functions is to use some kind of numerical procedure which yields approximate numerical values of the solution.

In the step-by-step integration approach the numerical values of the solution will be obtained at certain discrete points, $(t+\Delta t)$ and t where Δt is the length of the time interval. Assuming the solution is known at time$(t-\Delta t)$ the solution in steps with time interval Δt is by Taylor's series expansion

$$\{X(t)\} = \{X(t-\Delta t)\} + \Delta t\{\dot{X}(t-\Delta t)\} + \frac{\Delta t^2}{2!}\{\ddot{X}(t-\Delta t)\} + \frac{\Delta t^3}{3!}\{\dddot{X}(t-\Delta t)\} \quad (2)$$

where the terms containing derivatives of order higher than three have been neglected.

Differentiating equation (2) twice with respect to time and neglecting terms containing derivatives of order higher than three give

$$\{\dot{X}(t)\} = \{\dot{X}(t-\Delta t)\} + \Delta t\{\ddot{X}(t-\Delta t)\} + \frac{\Delta t^2}{2!}\{\dddot{X}(t-\Delta t)\}$$
$$\{\ddot{X}(t)\} = \{\ddot{X}(t-\Delta t)\} + \Delta t\{\dddot{X}(t-\Delta t)\} \quad (3)$$

Substituting the values of $\dddot{X}(t-\Delta t)$ from equation (2) into equation (3) gives the expressions for velocities and accelerations at time t in terms of velocities and accelerations at time $(t-\Delta t)$ and displacement at time t as follows :

$$\{\dot{X}(t)\} = \frac{3}{\Delta t}\{X(t)\} - \frac{3}{\Delta t}\{X(t-\Delta t)\} - 2\{\dot{X}(t-\Delta t)\}$$

$$-\frac{\Delta t}{2}\{\ddot{X}(t-\Delta t)\}$$

$$\{\ddot{X}(t)\} = \frac{6}{\Delta t^2}\{X(t)\} - \frac{6}{\Delta t^2}\{X(t-\Delta t)\} - \frac{6}{\Delta t}\{\dot{X}(t-\Delta t)\} - 2\{\ddot{X}(t-\Delta t)\} \quad (4)$$

Substitution of equation (4) into the equation (1) yields the desired equation in terms of one unknown, the displacement:

$$[K^*]\{X(t)\} = [P^*(t)] \quad (5)$$

where

$$[K^*] = [K] + \frac{3}{\Delta t}[C] + \frac{6}{\Delta t^2}[M]$$

$$[P^*(t)] = [P(t)] + [C]\{B(t)\} + [M]\{A(t)\}$$

$$\{A(t)\} = \frac{3}{\Delta t}\{X(t-\Delta t)\} + 2\{\dot{X}(t-\Delta t)\} + \frac{\Delta t}{2}\{\ddot{X}(t-\Delta t)\}$$

$$\{B(t)\} = \frac{6}{\Delta t^2}\{X(t-\Delta t)\} + \frac{6}{\Delta t}\{\dot{X}(t-\Delta t)\} + 2\{\ddot{X}(t-\Delta t)\}$$

Equation (5) may be solved for the unknown displacements at time t by Gaussian elimination (Ref.4).

3.3. Determination of Damping Values

A form of viscous damping, proportional to the mass and stiffness matrix, is given as follows:

$$[C] = \alpha[M] + \beta[K] \quad (6)$$

A significant portion of our experience with structural damping has been related to the frequencies and mode shapes of the system. Therefore it is worthwhile to relate the constants α and β in terms of equivalent modal damping.

The modal damping ratio λ_i for the i th mode is given in terms of α and β by

$$\lambda_i = \frac{\alpha}{2\omega_i} + \beta\frac{\omega_i}{2} \quad (7)$$

where ω_i is the angular frequency of the i th mode. For given values of α and β, the frequency ω^* which yields a minimum value of damping ratio λ^* is given by $\omega^* = \sqrt{\alpha/\beta}$. If the minimum damping ratio λ^* and the frequency ω^* are given, the damping constants α and β are calculated from the following relations

$$\alpha = \lambda^* \omega^*, \quad \beta = \lambda^* / \omega^* \quad (8)$$

The CSB frequencies for the first several modes for each of the zeroth to third shell harmonics are calculated and the frequencies corresponding to the first radial modes are obtained from the mode shapes. From these frequencies, constants of viscous damping, proportional to the mass and stiffness matrices, are determined.

Frequencies for the first 7 modes for each of the zeroth to third shell harmonics are shown in Table 1 and the frequencies corresponding to the first radial modes obtained from the mode shape are listed in Table 2. Using these frequencies, values of damping constants may be determined. A damping ratio of 4% is assumed for all elements of the CSB model. This damping ratio is in compliance with USNRC Reg. Guide 1.61 (Ref.5) which gives acceptable damping values for the seismic analysis of welded steel structures. Since safe shutdown earthquake and pipe break are both faulted conditions, the 4% value is applicable to the latter and is used herein. The damping constants which relate modal damping to the modal natural frequencies are obtained using equation (8) and are shown in Table 2.

Table 1. CSB Natural Frequencies

Mode	Shell Harmonic(cps)			
	0	1	2	3
1	56.82	85.53	50.16	48.82
2	163.10	118.99	115.83	83.08
3	211.36	207.61	145.69	132.69
4	326.54	290.90	190.82	166.71
5	334.36	308.43	250.17	186.58
6	386.13	343.97	296.05	233.30
7	405.91	358.08	331.01	275.14

Table 2. Frequencies and Damping Values Corresponding to First Radial Modes

Shell Harmonic	Frequencies(cps)		Damping Constants	
	1st Radial Mode	Mode No.	α	β
0	326.54	4	82.07	1.950E-5
1	85.53	1	21.50	7.443E-5
2	50.16	1	12.61	1.269E-4
3	48.82	1	12.27	1.304E-4

3.4. Forcing Functions

The dynamic loads on the CSB are developed from the time-varying radial pressure disturbances during an inlet pipe break. These are highly asymmetric in the circumferential direction and are caused by the expansion wave fronts and flow redistributions acting on the surface of the barrel. The radial pressures acting on the CSB may be defined as a series of harmonic functions(Fourier series). A pressure p is given by :

$$p(\theta) = \sum_{i=0}^{\infty} (A_i \cos i\theta + B_i \sin i\theta)$$

$$= A_0 + A_1\cos\theta + B_1\sin\theta + A_2\cos 2\theta + B_2\sin 2\theta + A_3\cos 3\theta + B_3\sin 3\theta + \cdots \quad (9)$$

Each term of the above series must be defined as a separate load step. A term is defined by the load coefficient (A_i or B_i), the number of harmonic waves and the symmetry condition(cos $i\theta$ or sin $i\theta$). Note that $i=0$ represents the axisymmetric term (A_0) and θ is the circumferential coordinate implied in the model. The load coefficient for the excitation pressure distribution is determined from the result of blowdown load time history analysis. The pressures at each circumferential location are computed relative to the pressure at an interior node.

Except for the first cosine and sine harmonics, all of the other higher order harmonics result in shell structural responses (Fig.3). The core support barrel shell model is excited at six axial elevations by an asymmetric pressure distribution defined at six equally spaced circumferential locations.

Fig.4 shows the delta pressure time histories for level 3 where inlet nozzle is located. There is a slight difference of delta pressure at six circumferential locations. The location of reference angle 0 degree goes from south to north and is parallel to the outlet nozzles. It means that the asymmetric loadings are not significant for this break. It is also anticipated from Fig.5, where all load coefficients except A_0 are almost zero. Fig.6 indicates that the smaller pressure disturbances are occurring on the lower part of CSB comparing with its upper part at the break location.

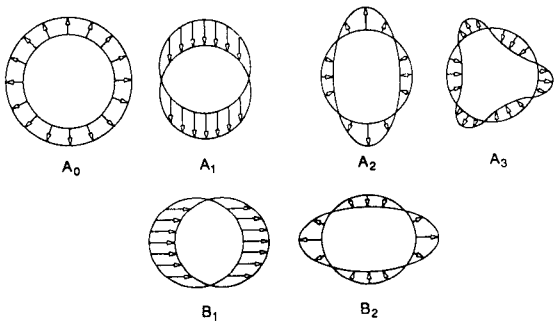

Fig. 3. CSB Differential Pressure Loading by Fourier Coefficient

4. Results and Discussion

Maximum values of principal stress and stress intensity for selected elements are tabulated in Tables 3 throuth 5. These stresses include secondary or self-limiting stresses which should be subtracted out before they are used. Also, the stresses

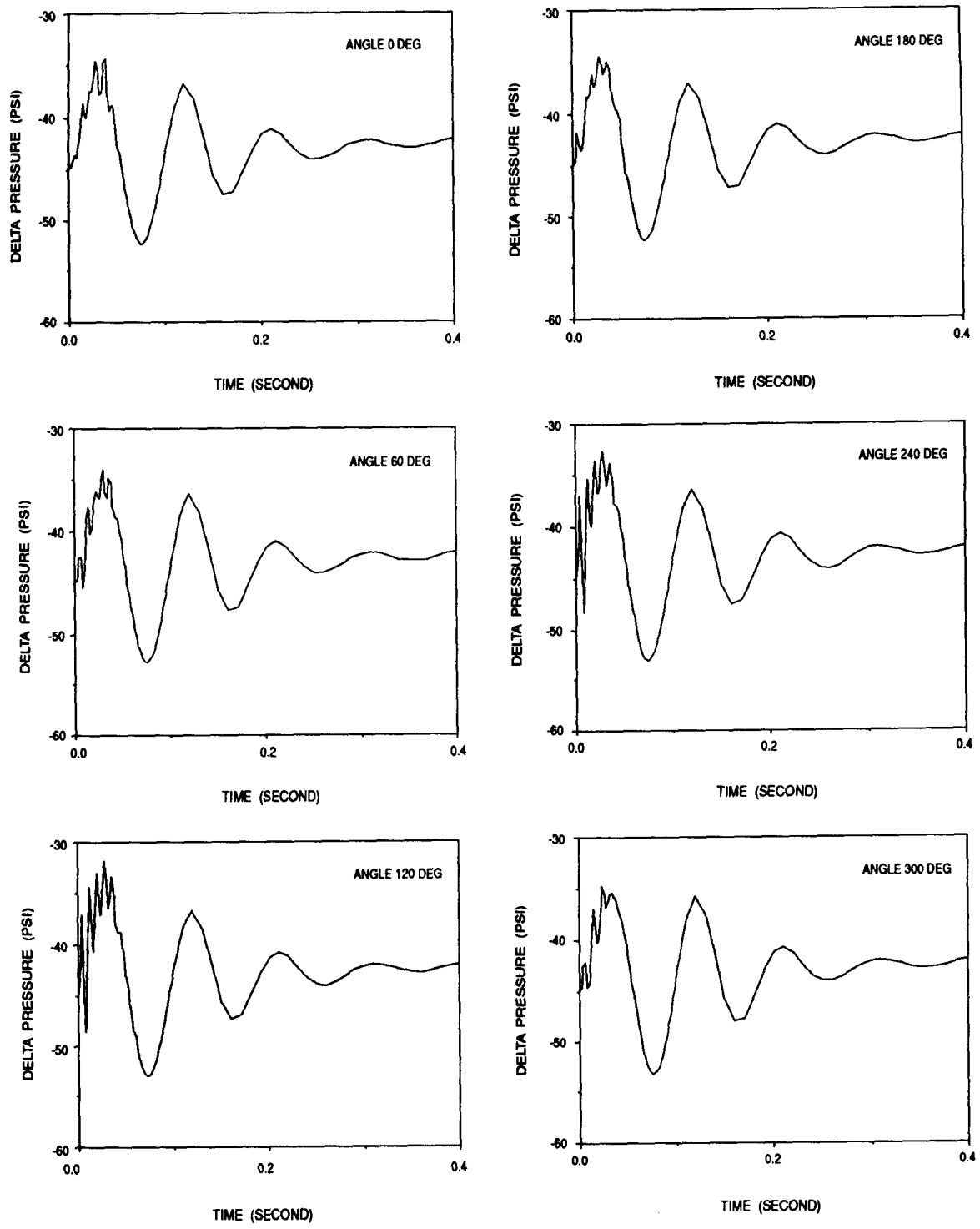

Fig. 4. Delta Pressure Time Histories for Level 3

due to the beam bending components (A_1+B_1) of the applied load are not included because they are considered in the analysis of the coupled internals and core (Ref.7). Therfore, stresses resulting from the horizontal and vertical pipe break analyses of the coupled internals and core must be combined with the results of this analysis to yield total stresses and stress intensities on the CSB.

The maximum stress intensities for each CSB cylinder are shown in Table 6. Also, the shell loads at the above locations for each Fourier term when maximum stress intensity occurs are calculated (Table 7). As expected, most of the responses come from coefficient A_0 which is the axisymmetric term.

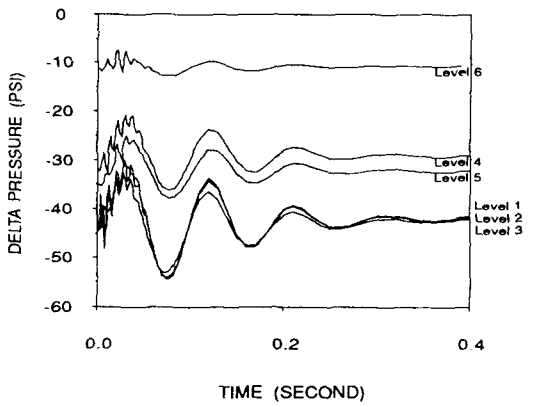

Fig. 6. Delta Pressure Time Histories of Each Level for Angle=240

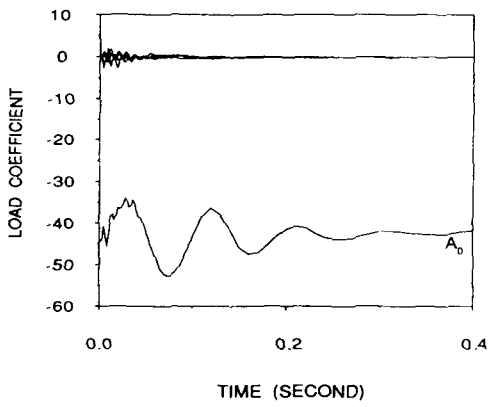

Fig. 5. Load Coefficient Time Histories at Level 3

The forces and moments for vertical and tangential components and for shear component are evaluated using the following equations (10) and (11), respectively, which are found easily by the trigonometric relations(Fig.7).

$$M(\theta), F(\theta) = A_0 + A_2 \cos 2\theta + B_2 \sin 2\theta + A_3 \cos 3\theta \quad (10)$$

$$M(\theta), F(\theta) = A_0 + A_2 \sin 2\theta + B_2 \cos 2\theta + A_3 \sin 3\theta \quad (11)$$

Table 3. Principal Stresses on Outer Surface

Node No.	SI (psi)	TIME (sec)	ANGLE (deg)	S2 (psi)	TIME (sec)	ANGLE (deg)
10	.172E+04	.148E−02	.100E+03	.106E+04	.420E−02	.110E+03
30	.195E+04	.125E−02	.000E+03	.340E+03	.268E−02	.180E+03
40	.171E+04	.120E−02	.000E+03	.348E+03	.300E−02	.180E+03
55	.146E+04	.118E−02	.110E+03	.491E+03	.950E−03	.110E+03
60	.167E+04	.118E−02	.100E+03	.528E+03	.715E−02	.700E+02
66	.168E+04	.118E−02	.290E+03	.542E+03	.100E−02	.110E+03
76	.149E+04	.118E−02	.300E+03	.390E+03	.235E−02	.180E+03
85	.110E+04	.570E−02	.100E+03	.457E+03	.248E−02	.180E+03
90	.106E+04	.340E−02	.180E+03	.384E+03	.250E−02	.180E+03
100	.731E+03	.488E−02	.100E+03	.139E+04	.653E−02	.180E+03

Table 4. Principal Stresses on Inner Surface

Node No.	SI (psi)	TIME (sec)	ANGLE (deg)	S2 (psi)	TIME (sec)	ANGLE (deg)
10	.252E+04	.160E−02	.110E+03	.189E+04	.178E−02	.110E+03
30	.196E+04	.123E−02	.180E+03	.471E+03	.308E−02	.180E+03
40	.171E+04	.120E−02	.180E+03	.482E+03	.308E−02	.180E+03
55	.139E+04	.118E−02	.100E+03	.400E+03	.720E−02	.110E+03
60	.197E+04	.115E−02	.290E+03	.922E+03	.100E−02	.110E+03
66	.164E+04	.120E−02	.600E+02	.396E+03	.139E−01	.180E+03
76	.156E+04	.120E−02	.600E+02	.575E+03	.189E−01	.180E+03
85	.111E+04	.803E−02	.180E+03	.393E+03	.115E−02	.110E+03
90	.110E+04	.343E−02	.700E+02	.547E+03	.135E−02	.100E+03
100	.131E+04	.630E−02	.180E+03	.119E+04	.630E−02	.180E+03

Table 5. Maximum Stress Intensities

NODE No.	OUTER SURFACE			INNER SURFACE		
	SI (psi)	TIME (sec)	ANGLE (deg)	SI (psi)	TIME (sec)	ANGLE (deg)
10	.261E+04	.163E−02	.900E+02	.252E+04	.160E−02	.110E+03
30	.195E+04	.125E−02	.000E+00	.196E+04	.123E−02	.180E+03
40	.171E+04	.120E−02	.000E+00	.171E+04	.120E−02	.180E+03
55	.146E+04	.118E−02	.110E+03	.139E+04	.118E−02	.100E+03
60	.178E+04	.125E−02	.180E+03	.197E+04	.115E−02	.290E+03
66	.168E+04	.118E−02	.290E+03	.164E+04	.120E−02	.600E+02
76	.150E+04	.790E−02	.250E+03	.156E+04	.120E−02	.600E+02
85	.113E+04	.795E−02	.230E+03	.115E+04	.793E−02	.180E+03
90	.110E+04	.790E−02	.180E+03	.110E+04	.343E−02	.700E+02
100	.189E+04	.640E−02	.180E+03	.131E+04	.630E−02	.180E+03

Table 6. Maximum Stress Intensities for Each CSB Cylinder

CSB Cylinder	SI (psi)	Surface	Time (sec)	Angle (deg)
Nozzle Cylinder	1960	Inner	.00123	180
Center Cylinder	1970	Inner	.00115	290
Lower Cylinder	1100	Inner	.00340	70

From the results of Tables 6 and 7, the shell loads when maximum stress intensity occurs are calculated using equations (10) and (11) and are summarized in Table 8. The loads are necessary for load combination under the Level D service condition. The stress intensities between the three breaks are compared in Table 9.

The allowable stress S_m of Type 304 stainless steel is 16200 psi at 650°F(Ref.6). For the 3 inch pipe break, the minimum stress margin not including beam mode contribution is

$$\frac{3.6\,S_m - S}{S} = \frac{3.6\,(16200) - 1970}{1970} = 28.6 \qquad (12)$$

Table 7. Shell Loads for Each Fourier Term

Cylinder	Coeff.	Moment(in-lb/in)			Force(lb/in)		
		vert.	tang.	shear	vert.	tang.	shear
Nozzle Cylinder	A_0	36.3	10.9	0.0	-299.7	-5843.0	0.0
	A_2	0.9	1.2	0.3	-3.7	-7.1	3.7
	B_2	0.0	0.0	0.0	0.0	0.0	0.0
	A_3	-1.5	-2.9	-0.5	3.5	3.6	-3.2
Center Cylinder	A_0	542.3	167.9	0.0	-954.0	-4763.0	0.0
	A_2	0.0	0.0	0.0	1.0	0.4	-0.1
	B_2	0.0	0.0	0.0	0.0	0.0	0.0
	A_3	0.0	-0.1	0.0	-1.1	0.1	-0.4
Lower Cylinder	A_0	74.2	22.3	0.0	-596.6	-2839.0	0.0
	A_2	-0.7	-0.2	0.0	8.4	0.1	5.8
	B_2	0.0	0.0	0.0	0.0	0.0	0.0
	A_3	0.0	0.0	0.0	-1.9	0.9	-2.0

Table 8. Dynamic Shell Loads of CSB due to 3 inch Break

Cylinder	Moment(in-lb/in)			Force(lb/in)		
	vert.	tang.	shear	vert.	tang.	shear
	SVM	STM	SSM	SVF	STF	SSF
Nozzle Cylinder	38.7	15.0	0.0	-306.9	-5853.7	0.0
Center Cylinder	542.3	168.0	0.0	-953.8	-4763.4	-0.1
Lower Cylinder	74.7	22.5	0.0	-601.4	-839.9	4.7

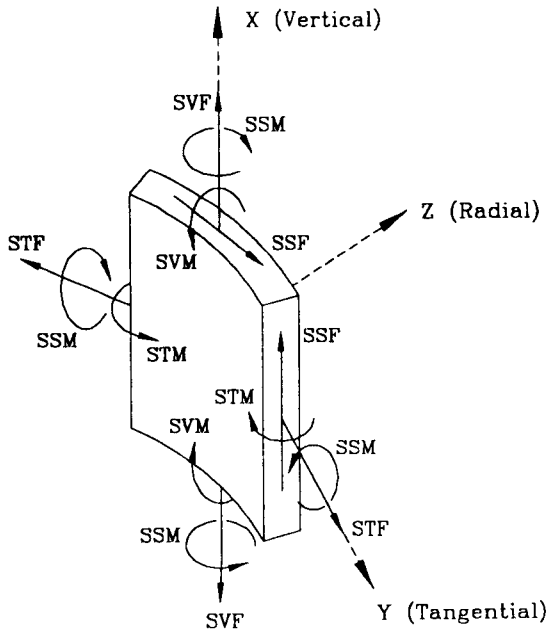

Fig. 7. Shell Forces of the Core Support Barrel

Thus, its effect is small enough to be negligible.

5. Conclusion

The CSB shell responses are calculated analytically for the 3 inch pressurizer spray line nozzle break which is the only inlet pipe break remaining in the primary side after the application of leak-before-break concept. They are compared with responses from 14 inch safety injection nozzle break and main coolant loop pipe break and are found to be so small. The calculated stress margin shows that shell responses due to pipe break are negligible for Level D service loading when leak-before-break concept is applied to the primary side piping systems with a diameter of 10 inches or over. It is concluded that the effect of tributary pipe breaks on the CSB shell responses may be no longer considered in the design of the reactor

Table 9. Comparison of Stress Intensities (psi)

Cylinder	3"BREAK	14"BREAK	MCL BREAK
Nozzle Cylinder	1960	12200	20703
Center Cylinder	1970	12200	32421
Lower Cylinder	1100	10400	17999

internals for the future nuclear power plant.

References

1. ASME Boiler and Pressure Vessel Code, Sec.III, Rules for Construction of Nuclear Power Plant Components, Division 1, Subsection NG, Core Support Structures (1989)
2. H. Kraus, *Thin Elastic Shells*, p.134, John Wiley and Sons, Inc.(1967)
3. E. L. Wilson and R. W. Clough, "Dynamic Response by Step-by-Step Matrix Analysis," Symposium on Use of Computers in Civil Engineering, Lisbon, Portugal (October 1962)
4. S. Ghosh and E. L. Wilson, "Dynamic Stress Analysis of Axisymmetric Structures Under Arbitrary Loading," Earthquake Engineering Research Center, University of California, Berkeley, California (September 1968)
5. USNRC Reg. Guide 1.61, "Damping Values for Seismic Design of Nuclear Power Plants" (October 1973)
6. ASME Boiler and Pressure Vessel Code, Sec.III, App.I (1989)
7. M. J. Jhung, et al., "Dynamic Analysis of Reactor Internals for the Tributary Pipe Breaks," Trans. SMiRT 11, Vol.J, pp.19–24 (August 1991)